Eradication of malaria may be achieved in such a system with a vaccine directed against conserved determinants, which may be naturally poorly immunogenic but may be rendered more effective by artificial methods. Vaccination strategies involving conserved antigens must be based on the R_0 of the strain with the highest transmissibility, as is the case for the measles-mumps-rubella vaccine (*1*), where the R_0 of measles determines the requisite vaccine coverage. At the low values of R_0 indicated by our analysis of epidemiological data, malaria may be easier to control by mass vaccination (*29*) than expected.

REFERENCES AND NOTES

1. R. M. Anderson and R. M. May, *Infectious Diseases of Humans: Dynamics and Control* (Oxford Univ. Press, Oxford, 1991).
2. A. R. McLean and R. M. Anderson, *Epidemiol. Infect.* **100**, 111 (1988).
3. D. J. Nokes and R. M. Anderson, *Lancet* i, 1441 (1987).
4. L. Molineaux and G. Gramiccia, *The Garki Project* (World Health Organisation, Geneva, 1980).
5. B. M. Greenwood, K. Marsh, R. W. Snow, *Parasitol. Today* **7**, 277 (1991).
6. J. A. Cattani *et al.*, *Am. J. Trop. Med. Hyg.* **35** (no. 1), 3 (1986).
7. K. Marsh, *Parasitol. Today* **104**, 553 (1992).
8. R. C. Muirhead-Thomson, *Trans. R. Soc. Trop. Med. Hyg.* **48**, 208 (1954).
9. F. B. Bang *et al.*, *ibid.* **40**, 809 (1947).
10. J. de Zulueta *et al.*, *East Afr. Med. J.* **38**, 1 (1961).
11. *Report on the Pare-Taveta Malaria Scheme 1954–1959* (East Africa High Commission, Dar es Salaam, Tanzania, 1960).
12. P. M. Graves *et al.*, *Parasitology* **96**, 251 (1988).
13. D. B. Wilson and M. E. Wilson, *East Afr. Med. J.* **39**, 593 (1962).
14. G. Davidson and C. C. Draper, *Trans. R. Soc. Trop. Med. Hyg.* **47**, 522 (1953).
15. F. D. Gibson, *West Afr. Med. J.* **7**, 170 (1958).
16. M. D. Young and T. H. Johnson, *J. Nat. Malar. Soc.* **8**, 247 (1949).
17. This applies also to other measures of risk of infection, such as the entomological inoculation rate (high entomological inoculation rate does not indicate that R_0 is high).
18. K. P. Day and K. Marsh, *Parasitol. Today* **6**, A68 (1990).
19. T. R. Burkot *et al.*, *Am. J. Trop. Med. Hyg.* **39** (no. 2), 135 (1988).
20. C. N. M. Mbogo *et al.*, *ibid.* **49(no. 2)**, 245 (1993).
21. S. W. Lindsay *et al.*, *Ann. Trop. Med. Parasitol.* **84**, 555 (1990).
22. K. P. Forsyth *et al.*, *Am. J. Trop. Med. Hyg.* **41**, 259 (1989).
23. D. Walliker, *Science* **236**, 1661 (1987).
24. K. Marsh and R. J. Howard, *ibid.* **231**, 150 (1986).
25. C. I. Newbold, R. Pinches, D. J. Roberts, K. Marsh, *Exp. Parasitol.* **75**, 281 (1992).
26. P. Deloron and C. Chougnet, *Parasitol. Today* **8**, 375 (1992).
27. K. Marsh *et al.*, *Trans. R. Soc. Trop. Med. Hyg.* **83**, 293 (1989).
28. D. J. Roberts *et al.*, *Nature* **357**, 689 (1992).
29. R. M. Anderson, R. M. May, S. Gupta, *Parasitology* **99**, S59 (1989).
30. We use an age-structured mathematical model for malaria transmission with overlapping categories of exposed, x, and immune, z, hosts. Nonimmunes acquire infection from contact with infectious mosquitoes, present in proportion y in the vector population, and become immune. Immunity is lost at rate h. Once exposed, however, an individual remains in the exposed category for life; hence, the rate of loss of exposed individuals is identical to the community death rate, μ. If infection induces lifelong immunity, then $h = \mu$. The transmission system can be described by the following set of partial differential equations

$$\frac{\delta x}{\delta a} + \frac{\delta x}{\delta t} = m\alpha b(1 - x)y - \mu x$$

$$\frac{\delta z}{\delta a} + \frac{\delta z}{\delta t} = m\alpha b(1 - z)y - hz$$

$$\frac{dy}{dt} = m\alpha^2 bD(1 - y)y[1 - \int \mu z(a)e^{-\mu a}\partial a] - \frac{1}{L_M}y$$

Here, m is the number of mosquitoes per human host, α is the mosquito biting rate, b is the probability of transmission from vector to host, L_M is the average life-span of the mosquito, and D is measured in the human host. Within this system, $R_0 = m\alpha^2 bDL_M$ [J. L. Aron and R. M. May, in *Population Dynamics of Infectious Diseases: Theory and Applications*, R. M. Anderson, Ed. (Chapman and Hall, London, 1982), pp. 139–179].
31. We performed agglutination assays on plasma samples using lines selected for the expression of agglutination phenotypes (by binding to C32 amelanotic melanoma cells) using methods as described [K. P. Day *et al.*, *Proc. Natl. Acad. Sci. U.S.A.* **90**, 8292 (1993)]. Trophozoite-infected cells of the above lines were reacted with sera as described (*22*) from a cross-sectional survey involving the following numbers of individuals (n) in each age class: for 1 year of age with isolates 1776, HB3, 1934, and 1935 (n = 3) and with isolate 1917 (n = 2); for age 1 to 4 years with isolates 1776, HB3, and 1917 (n = 18) and with isolates 1934 and 1935 (n = 17); for 5 to 9 years with isolates 1776, HB3, and 1934 (n = 16), with isolate 1917 (n = 14), and with isolate 1935 (n = 13); for 10 to 14 years with isolates 1776, HB3, and 1934 (n = 11), with isolate 1917 (n = 10), and with isolate 1935 (n = 9); for 15 to 19 years with isolates 1776, HB3, 1934, and 1917 (n = 11) and with isolate 1935 (n = 10); for 20 to 29 years with isolates 1776, HB3, 1934, and 1917 (n = 18) and with isolate 1935 (n = 15); and for ≥30 years with isolates 1776, HB3, and 1934 (n = 16), with isolate 1917 (n = 15), and with isolate 1935 (n = 13).
32. To determine whether there was a correlation with R_0 in the correspondence of the distribution generated by the model with the observed pattern, we used a simple inverse measure: $S = \Sigma$(observed pattern − expected pattern)^2, of the "goodness of fit," where S is the average squared difference. In Fig. 3B, this measure is plotted with respect to R_0, showing a best fit around values between 6 and 7. Maximum likelihood estimates of R_0 for each strain (assuming that each confers lifelong immunity) were in the range of 2 to 10. Note that there may be some bias in these values because of host heterogeneity.

33. We thank R. M. May and A. V. S. Hill for comments. Supported by the Wellcome Trust, the Leverhulme Trust, and the UNDP–World Bank–World Health Organisation Special Programme for Research and Training in Tropical Diseases.

27 September 1993; accepted 10 December 1993

Diverse Essential Functions Revealed by Complementing Yeast Calmodulin Mutants

Yoshikazu Ohya* and David Botstein

Calmodulin, a cytoplasmic calcium-binding protein, is indispensable for eukaryotic cell growth. Examination of 14 temperature-sensitive yeast mutants bearing one or more phenylalanine to alanine substitutions in the single essential calmodulin gene of yeast (*CMD1*) revealed diverse essential functions. Mutations could be classified into four intragenic complementation groups. Each group showed different characteristic functional defects in actin organization, calmodulin localization, nuclear division, or bud emergence. Phenylalanine residues implicated in calmodulin localization and nuclear division are located in the amino-terminal half of the protein, whereas those implicated in actin organization and bud emergence are located in the carboxyl-terminal half.

Calmodulin is a Ca^{2+}-binding protein implicated in many functions in eukaryotic cells (*1*). It interacts with more than 20 different proteins including several metabolic enzymes, protein kinases, a protein phosphatase, ion transporters, receptors, motor proteins, and cytoskeletal components (*1*, *2*). Budding yeast (*Saccharomyces cerevisiae*) contains a single gene encoding calmodulin (*CMD1*), which is essential for cell growth (*3*). Calmodulins from yeast and vertebrates have structural, biochemical, and biophysical similarity (*4*) and are functionally conserved (*5*). Extensive analysis of two temperature-sensitive mutations (*cmd1-1* and *cmd1-101*) indicated that a defect in mitosis (*6*, *7*)—specifically, impaired spindle pole body (SPB) function (*6*)—is responsible for the temperature-sensitive lethality. However, the finding of many functions unrelated to mitosis in vitro indicated that nuclear division might not be the only essential function requiring calmodulin (*8*).

If calmodulin indeed has diverse essential roles, it might be possible to find additional conditional-lethal mutations in *CMD1* that impair each of these essential functions. Conversely, identification of several distinct defects specified by different *cmd1* mutations would serve to demonstrate the multiple essential roles of calmodulin in cell growth. Mutations were obtained by specific alteration of the phenylalanine residues in calmodulin, which were predicted

Department of Genetics, Stanford University School of Medicine, Stanford, CA 94305, USA.

*Present address Department of Plant Sciences, Graduate School of Science, University of Tokyo, Hongo, Tokyo 113, Japan.

to contribute strongly to interaction of calmodulin with its several protein ligands. All eight Phe residues in yeast calmodulin are conserved in mammalian calmodulin (*3*). The three-dimensional structure of calmodulin bound to a calmodulin-binding peptide shows that seven out of the eight Phe residues can interact with the peptide (*9*). We systematically replaced each of the phenylalanines with alanine in the expectation that this would eliminate the hydrophobic effect of the side chain beyond the β carbon with minimal disturbance of the main chain conformation. Among 33 site-directed mutations that contain single and multiple Phe (F) to Ala (A) changes, 14 result in temperature-sensitive phenotypes (*10*). This set of the conditional lethal mutations provided an opportunity to demonstrate the multiple functions of calmodulin in cell growth.

We report here intragenic complementation among the calmodulin mutants, as observed in diploids formed by reciprocal matings between strains carrying different *cmd1-ts* alleles. Diploid strains homozygous for the parental *cmd1* alleles did not grow at the restrictive temperature, but diploids bearing different recessive alleles (heteroallelic diploids) often were able to grow. The pattern of growth at restrictive temperature for all combinations of four recessive alleles (along with a wild-type control) revealed four intragenic complementation groups (Fig. 1) (*11*). The growth rates of many of these heteroallelic diploids were almost the same as those of the wild-type strains (*12*). Heteroallelic diploids constructed with *cmd1-233* grew relatively slowly because of the partial dominance of *cmd1-233* (*12*); however, this dominance was not so severe as to make analysis difficult.

The four complementation groups along with the Phe to Ala changes that comprise the complementing alleles are listed in Table 1. Members of the *cmd1A* group all contain the F92A mutation, and members of the *cmd1C* group have two changes (F65A and F68A) in common. The remaining patterns are not so simply interpretable: F12A, for example, is common to many groups.

Intragenic complementation can sometimes be observed among mutations in a multifunctional gene. For example, the yeast *HIS4* protein is a multifunctional protein that catalyzes three different enzymatic steps in histidine biosynthesis; mutations affecting only one of these steps complement mutations affecting only one of the others (*13*). Our intragenic complementation results are compatible with this view, although the structural domains in calmodulin may not be as simply separable as the domains of the *HIS4* product. Of the many alternative mechanisms that might account for intragenic complementation, those that involve interactions of identical subunits seem unlikely, since yeast calmodulin, like the mammalian protein, is present as a monomer in a solution (*14*). Analysis of the level of calmodulin protein and stability of the protein in vivo makes it unlikely that the difference is due simply to differing levels of protein (*15*). Despite our inability at this time to further elucidate the molecular mechanisms by which the different calmodulin mutants differ in their activity in vivo, the most likely supposition is that calmodulin, as a monomer, undergoes a diverse set of interactions corresponding to different essential functions.

We analyzed phenotypes of mutations representing the various complementation groups, expecting that each might correspond to a distinct essential function requiring calmodulin. Two groups of the calmodulin mutants showed cell cycle arrest phenotypes. The *cmd1-239* cells (a member of the *cmd1C* group) had defects in nuclear division. After 3 hours or more of incubation the cells stopped growing, and more than 90% of the cells contained a large bud (Fig. 2D). Analysis of cells labeled with propidium iodide in a fluorescence-activated cell sorter (FACS) revealed that the arrested cells had replicated their DNA (*15*). The nucleus in these cells had not divided and was stuck in the neck between the bud and the mother (Fig. 3, G and I). Two types of microtubule morphology were observed in these mutant cells. The major type (70%) appeared to represent one SPB and several elongated cytoplasmic microtubules (Fig. 3F). The minor type (30%) was more consistent with two SPBs connected by a short spindle (Fig. 3H), and one of the SPBs was apparently not associated with the nuclear DNA (Fig. 3I). The mitotic arrest phenotype of *cmd1-239* is indistinguishable from that previously reported for *cmd1-101* cells (*6*).

The *cmd1-233* cells (*cmd1D*) also showed a cell cycle arrest, but at a different point in the cell cycle. They did not form buds at the restrictive temperature. After 4 hours of incubation at 37°C, more than 90% of the cells arrested as unbudded cells. The cells continued to enlarge (Fig. 2E), suggesting that macromolecular synthesis continued long after arrest. FACS analysis showed that most of the DNA was replicated in *cmd1-233* cells (*15*). Divided nuclei were rarely observed after 4 hours of incubation. However, after 8 hours or more of incubation two or more nuclei could be seen in many cells, still in the absence of a visible bud (Fig. 2E). Involvement of calmodulin in bud emergence is consistent with the observation that a mutation in yeast *MYO2* gene, a yeast gene specifying a myosin with putative calmodulin binding sites, also displays a similar defect in bud emergence (*16*). The calmodulin made from *cmd1-233* mutant gene may be unable to interact with Myo2p, thereby causing a budding defect.

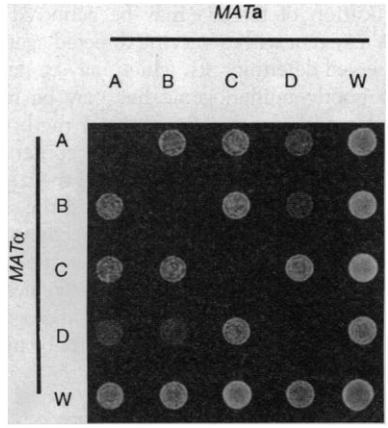

Fig. 1. Intragenic complementation among temperature-sensitive calmodulin mutations. The alleles used were as follows: A, *cmd1-226*; B, *cmd1-228*; C, *cmd1-239*; and D, *cmd1-233*. The constituent changes in each allele are listed in Table 1. Diploids were selected with complementary auxotrophic markers in the strains, and the growth shown is on rich (YEP-glucose) medium at 37°C onto which diploids were inoculated with a multipoint inoculation device. W, wild type.

Mutations in the remaining calmodulin complementation groups did not show uniform cell cycle arrest at the nonpermissive temperature. Cells carrying the *cmd1-226* allele (*cmd1A*) displayed abnormal actin organization. In wild-type cells (Fig. 3A) many actin cortical patches are observed in growing buds and, at cytokinesis, in the neck between mother and daughter cells

Table 1. Complementation groups of the *cmd1* mutations. Diploids were constructed by all possible pairwise crosses of the 14 *cmd1-ts* strains. Temperature sensitivity of these diploids examined at 37°C revealed four complementation groups of the recessive mutations. The other seven temperature-sensitive mutations that are not included in this table are either dominant (*cmd1-242* and *cmd1-247*) or contain multiple defects (*cmd1-234*, *cmd1-235*, *cmd1-240*, *cmd1-251*, and *cmd1-252*) as judged from their inability to complement mutations in more than one of the four groups.

Group	Allele	Mutation
cmd1A	*cmd1-226*	F92A
	cmd1-232	F12A F92A
cmd1B	*cmd1-228*	F12A F16A F19A
cmd1C	*cmd1-239*	F65A F68A
	cmd1-250	F12A F65A F68A
cmd1D	*cmd1-231*	F12A F89A
	cmd1-233	F12A F140A

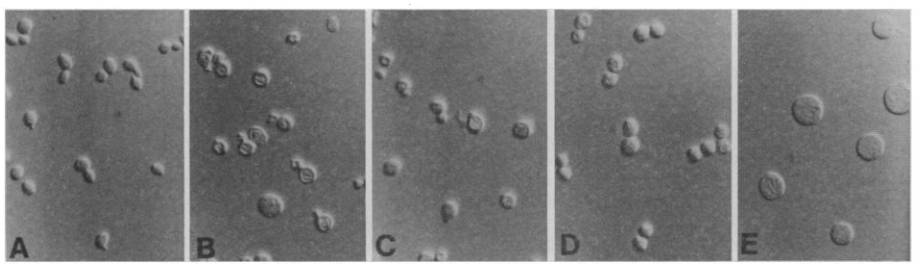

Fig. 2. Differential interference contrast (Nomarsky) images of wild-type and *cmd1* cells. Cells of the wild-type control (**A**), *cmd1-226* (**B**), *cmd1-228* (**C**), *cmd1-239* (**D**), and *cmd1-233* (**E**) were grown at 25°C. Cell morphologies were observed under the microscope after incubation for 4 hours (A through D) or 8 hours (E) at 37°C.

(*17*). Actin cables are visible mainly in the mother cells. At the permissive temperature, *cmd1-226* cells grew more slowly than wild-type cells and frequently contained delocalized actin. The phenotype was more obvious at the restrictive temperature. After 90 min of incubation, more than 95% of the cells lost the localized cortical patches of actin in the bud (Fig. 3B), and actin cables were no longer visible. Two lines of evidence indicate that the delocalization of actin is a primary defect caused by the mutations rather than a secondary effect caused by a cell cycle–dependent event. First, even after a shorter period of incubation (30 min) at 33°C, we observed abnormal distribution of actin in most (84%) of the cells. Second, unlike many of the other calmodulin mutants, *cmd1-226* cells did not show any cell cycle–specific arrest phenotypes. Asynchronous cultures of the *cmd1-226* cells stopped growing after 4 hours of incubation at 37°C with a distribution of morphology apparently representative of all stages of the cell cycle (Fig. 2B).

Wild-type calmodulin concentrates at the growing portion of the bud early in the cell cycle and localizes mainly at the neck between mother and daughter cells at cytokinesis (Fig. 3D) (*18*). The molecular basis for this intracellular distribution of calmodulin is still uncertain. Nevertheless, it is clear that cells carrying the *cmd1-228* allele (*cmd1B*) have lost this polarized localization of calmodulin. At the restrictive temperature, most of the *cmd1-228* cells contained diffused calmodulin throughout the cells. Disappearance of specific localization of calmodulin was also seen even after 30 min of incubation at the nonpermissive temperature (Fig. 3E). Actin morphology was well preserved in these cells (Fig. 3C), indicating that overall cell polarity was still maintained. The *cmd1-228* cells stopped growing after 4 hours of incubation at 37°C with a distribution of morphology apparently representative of all stages of the cell cycle (Fig. 2C); at this time they had also suffered substantial loss of viability.

Analyses of the remaining temperature-sensitive calmodulin mutants revealed that the phenotype of each was related to its complementation group and sometimes to the presence of one or more particular Phe to Ala changes. Specifically, all temperature-sensitive strains bearing the F92A mutation (*cmd1-226* and *cmd1-232*; the *cmd1A* group) had the actin organization defect; all F16A F19A mutants (*cmd1-228*, and others including *cmd1-234*, *cmd1-235*, *cmd1-251*, and *cmd1-252*, all of which fail to complement *cmd1-228* and thus lack the *cmd1B* function) showed loss of localization of calmodulin to the buds and reduced viability; all F65A F68A mutants (*cmd1-239* and *cmd1-250*; the *cmd1C* group) had the nuclear division defect; all F89A and F140A mutants (*cmd1-231*, *cmd1-233*, and others including *cmd1-240*, *cmd1-242*, and *cmd1-247*) had the bud emergence defect.

Our interpretation of these data is that particular Phe residues can be assigned to several diverse calmodulin functions affecting progression of the cell cycle. F16 and F19 appear to be determinants of the subcellular localization of calmodulin to buds; F65 and F68 are implicated in nuclear division; F89 and F140 are implicated in bud emergence; F92 is somehow involved in actin organization. The remaining Phe residue, F12, seems to act mainly in concert with other Phe residues. The F12A mutation is necessary to express phenotypes of either the F16A F19A, F89A, or F140A mutation: The F16A F19A, F89A, or F140A mutations alone have no deleterious phenotype (*10*). Moreover, addition of F12A to *cmd1-239* (F65A F68A) and *cmd1-226* (F92A) produced *cmd1-250* and *cmd1-232*, respectively, with no alteration in their complementation group (Table 1). Diversity of functional consequences of calmodulin mutations has been observed previously among calmodulin mutants of *Paramecium* (*19*). Although these mutations have minimal growth defects, mutations in the NH_2-terminal half in the molecule underreact to stimuli, whereas the mutations in the COOH-terminal half overreact to stimuli.

In conclusion, diverse functions of calmodulin could be revealed as intragenic complementation groups, even though the complementing alleles consisted of multiple mutations changing Phe residues to Ala. The power of intragenic complementation analysis lies in its ability to separate and to identify each function of this multifunctional protein. This technique might serve also as a tool to dissect the cellular processes regulated by other multifunctional proteins. We hope to identify the protein ligands of calmodulin that participate in each of its diverse functions, and expect that each ligand may bind to a different subset of phenylalanines in calmodulin.

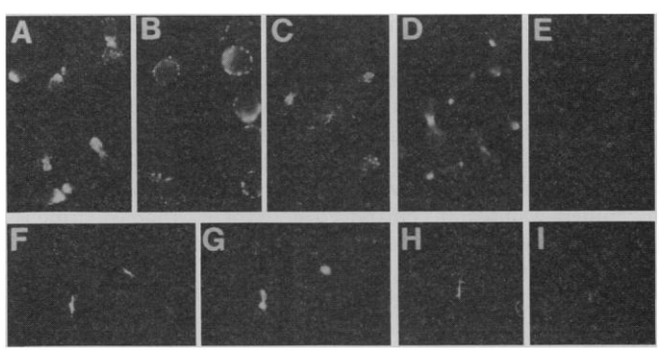

Fig. 3. Fluorescence micrographs of the wild-type controls and *cmd1* mutant cells. Diploid cells of the wild-type control were grown at 25°C. Homozygous *cmd1* diploid cells were incubated for 90 min at 37°C (*cmd1-226/cmd1-226*), for 30 min at 33°C (*cmd1-228/cmd1-228*), or for 4 hours at 37°C (*cmd1-239/cmd1-239*). Actin morphologies of the wild-type (**A**), *cmd1-226/cmd1-226* (**B**), and *cmd1-228/cmd1-228* (**C**) cells were observed after the cells were stained with rhodamine-phalloidin (*20*). Indirect immunofluorescence microscopy (*20*) was used to visualize localized calmodulin distribution of wild-type (**D**) and *cmd1-228/cmd1-228* (**E**) cells, and morphologies of microtubule in *cmd1-239/cmd1-239* cells (**F** and **H**). Nuclear DNA of *cmd1-239/cmd1-239* cells (**G** and **I**) was stained with 4′ 6-diamidino-2-phenylindole. Pairs (F and G and H and I) show the same cells.

REFERENCES AND NOTES

1. P. Cohen and C. B. Klee, *Calmodulin: Molecular Aspects of Cellular Regulation* (Elsevier, Amsterdam, Netherlands, 1988), vol. 5.
2. J. A. Airey, M. M. Grinsell, L. R. Jones, J. L. Sutko, D. Witcher, *Biochemistry* **32**, 5739 (1993); E. San Jose, A. Benguria, P. Geller, A. Villalobo, *J. Biol. Chem.* **267**, 15237 (1992); H. J. Matthies, R. J.

Miller, H. C. Palfrey, *ibid.* **268**, 11176 (1993); E. M. Espreafico *et al.*, *J. Cell Biol.* **119**, 1541 (1992).
3. T. N. Davis, M. S. Urdea, F. R. Masiarz, J. Thorner, *Cell* **47**, 423 (1986).
4. M. A. Starovasnik, T. N. Davis, R. E. Klevit, *Biochemistry* **32**, 3261 (1993).
5. Y. Ohya and Y. Anraku, *Biochem. Biophys. Res. Commun.* **158**, 541 (1989); T. N. Davis and J. Thorner, *Proc. Natl. Acad. Sci. U.S.A.* **86**, 7909 (1989).
6. G.-H. Sun, A. Hirata, Y. Ohya, Y. Anraku, *J. Cell Biol.* **119**, 1625 (1992).
7. T. N. Davis, *ibid.* **118**, 607 (1992). Calmodulin is implicated in nuclear division in other organisms [K. P. Lu, S. A. Osmani, A. H. Osmani, A. R. Means, *J. Cell Biol.* **121**, 621 (1993); C. D. Rasmussen and A. R. Means, *EMBO J.* **8**, 73 (1989)].
8. T. N. Davis, *Cell Calcium* **13**, 435 (1992); Y. Ohya and Y. Anraku, *ibid.*, p. 445.
9. M. Ikura *et al.*, *Science* **256**, 632 (1992); W. E. Meador, A. R. Means, F. A. Quiocho, *ibid.* **257**, 1251 (1992).
10. Y. Ohya and D. Botstein, in preparation. Temperature-sensitive *cmd1* alleles used in this study were *cmd1-226* (F92A), *cmd1-228* (F12A F16A F19A), *cmd1-231* (F12A F89A), *cmd1-232* (F12A F92A), *cmd1-233* (F12A F140A), *cmd1-234* (F16A F19A F65A), *cmd1-235* (F16A F19A F68A), *cmd1-239* (F65A F68A), *cmd1-240* (F65A F89A), *cmd1-242* (F65A F140A), *cmd1-247* (F89A F140A), *cmd1-250* (F12A F65A F68A), *cmd1-251* (F12A F16A F19A F68A), and *cmd1-252* (F12A F16A F19A F65A).
11. The ability to grow at restrictive temperature is not due to recombination or gene conversion. Using allele-specific polymerase chain reaction primers, we could routinely detect both alleles in the diploids.
12. Exponential growth rates were measured in rich (YEP-glucose) medium at the restrictive temperature (37°C). Many heteroallelic diploid strains including *cmd1-226/cmd1-228, cmd1-226/cmd1-239, cmd1-226/CMD1, cmd1-228/cmd1-239, cmd1-228/CMD1*, and *cmd1-239/CMD1* have growth rates (1.9 to 2.0 hour doubling times) the same as those of the wild-type diploid control (1.9 hours). The other heteroallelic strains have slightly slower growth rates: *cmd1-226/cmd1-233* (2.4 hours), *cmd1-228/cmd1-233* (2.4 hours), *cmd1-239/cmd1-233* (2.3 hours), and *cmd1-233/CMD1* (2.2 hours).
13. G. R. Fink, *Genetics* **53**, 445 (1966); R. Bigelis, J. Keesey, G. R. Fink, in *ICN-UCLA Symposia on Molecular and Cellular Biology*, G. Wilcox, J. Abelson, C. Fox, Eds. (Liss, New York, 1977), vol. 8, pp. 179–188; L. J. Reha-Krants, *Genetics* **124**, 213 (1990); M. J. Schlesinger, A. Torriani, C. Levinthal, *Cold Spring Harbor Symp. Quant. Biol.* **28**, 539 (1964).
14. Y. Ohya, I. Uno, T. Ishikawa, Y. Anraku, *Eur. J. Biochem.* **168**, 13 (1987); Y. Ohya and Y. Anraku, unpublished data.
15. Y. Ohya and D. Botstein, unpublished data. A full description of the properties of these mutants is in preparation.
16. G. C. Johnson, J. A. Prendergast, R. A. Singer, *J. Cell Biol.* **113**, 539 (1991).
17. A. E. M. Adams and J. Pringle, *ibid.* **98**, 934 (1984).
18. G.-H. Sun, Y. Ohya, Y. Anraku, *Protoplasma* **166**, 110 (1992); S. E. Brockerhoff and T. N. Davis, *J. Cell Biol.* **118**, 619 (1992).
19. J. A. Kink *et al.*, *Cell* **62**, 165 (1990).
20. J. R. Pringle *et al.*, *Methods Cell Biol.* **31**, 357 (1989).
21. Supported by grants to D.B. from NIH (GM46406 and GM46888). Y.O. was the recipient of a long-term fellowship from the Human Frontier Science Program Organization, Strasbourg, France.

6 October 1993; accepted 28 December 1993

Agmatine: An Endogenous Clonidine-Displacing Substance in the Brain

Gen Li, S. Regunathan, Colin J. Barrow, Jamshid Eshraghi, Raymond Cooper, Donald J. Reis*

Clonidine, an antihypertensive drug, binds to α_2-adrenergic and imidazoline receptors. The endogenous ligand for imidazoline receptors may be a clonidine-displacing substance, a small molecule isolated from bovine brain. This clonidine-displacing substance was purified and determined by mass spectroscopy to be agmatine (decarboxylated arginine), heretofore not detected in brain. Agmatine binds to α_2-adrenergic and imidazoline receptors and stimulates release of catecholamines from adrenal chromaffin cells. Its biosynthetic enzyme, arginine decarboxylase, is present in brain. Agmatine, locally synthesized, is an endogenous agonist at imidazoline receptors, a noncatecholamine ligand at α_2-adrenergic receptors and may act as a neurotransmitter.

In 1984, Atlas and Burstein (*1*) partially purified a substance from calf brain that displaced binding of clonidine, an antihypertensive drug, to α_2-adrenergic receptors of rat brain. This clonidine-displacing substance (CDS) was not a catecholamine nor a peptide and had an estimated mass of 520 daltons. It was subsequently discovered that CDS, like clonidine, would also bind to a nonadrenergic binding site, the imidazoline receptor (I receptor) (*2–4*), which is believed to mediate the hypotensive actions of clonidine and allied agents (*5*). I receptors exist in two major subclasses, I_1 and I_2 (*6*), which differ from α_2-adrenergic receptors and each other with respect to selectivity for ligands, structure, and regional, cellular, and subcellular localizations (*7, 8*). The endogenous ligand of I receptors is not known. However, the fact that CDS binds to all I receptors (*3, 8*) and is bioactive (*9, 10*) suggested that CDS may fill this role, and we sought to establish its structure.

We partially purified CDS from bovine brain using displacement of [^{3}H]*p*-aminoclonidine ([^{3}H]PAC) from rat cerebral cortical membranes to track its activity (*8, 11*). Fresh bovine brains were homogenized in chilled water and centrifuged and the supernatant was precipitated in 70% ethanol. After condensation on a rotatory evaporator and centrifugation, the supernatant was passed through a Dowex 50 (H^+) column eluting with 3 N hydrochloric acid. This step was followed by C_{18} reversed-phase high-performance liquid chromatography (HPLC) eluting with acetic acid (25 mM). Further purification (*12*) was achieved with size-exclusion HPLC with a Bio-Rad SEC 125 column from which CDS was eluted in a fraction that indicated that its molecular mass was less than 300 daltons. CDS tested positive with a ninhydrin spray reagent on thin-layer chromatography. At this stage, CDS contained no ultraviolet chromophore over 200 nm, was a highly polar low molecular weight compound containing an amine functionality, and was contained in a mixture of compounds.

Further attempts to purify CDS directly were unsuccessful, and we therefore isolated CDS in its derivatized form (*13*). Derivatization of the enriched active fraction with 9-fluorenylmethyl chloroformate (FMOC-Cl) generated a mixture of compounds stable under most purification conditions. Although binding was lost on derivatization, it was regained after base hydrolysis to release the free amine. Sequential C_{18}-column chromatography of the derivatized mixture, which monitored the biological activity enrichment by release of free amine from a subsample of each fraction, yielded a single peak on C_{18} HPLC that coeluted with authentic FMOC-agmatine. Subjecting the natural purified FMOC-CDS derivative to electrospray mass spectroscopy–mass spectroscopy (MSMS) analysis gave results identical to those obtained for authentic FMOC-agmatine, which confirms that agmatine is the CDS compound isolated (Fig. 1). We quantitated the amount of agmatine in weighed amounts of bovine brain by derivatization to FMOC-Cl of a fraction (based on 200 U of CDS activity). The quantity of FMOC-agmatine present was determined from a standard curve generated by plotting ultraviolet intensity as a function of FMOC-agmatine concentration. In this way, the amount of agmatine in bovine brain was found to be 1.5 to 3.0 nmol per gram of tissue (0.2 to 0.4 μg/g),

G. Li, S. Regunathan, D. J. Reis, Division of Neurobiology, Department of Neurology and Neuroscience, Cornell University Medical College, 411 East 69 Street, New York, NY 10021, USA.
C. J. Barrow, J. Eshraghi, R. Cooper, Sterling Winthrop Pharmaceuticals Research Division, 25 Great Valley Parkway, Malvern, PA 19355, USA.
*To whom correspondence should be addressed.